# We are IntechOpen, the world's leading publisher of Open Access books
# Built by scientists, for scientists

## 6,900
Open access books available

## 185,000
International authors and editors

## 200M
Downloads

Our authors are among the

## 154
Countries delivered to

## TOP 1%
most cited scientists

## 12.2%
Contributors from top 500 universities

CLARIVATE ANALYTICS
BOOK CITATION INDEX
INDEXED

**WEB OF SCIENCE**™

Selection of our books indexed in the Book Citation Index
in Web of Science™ Core Collection (BKCI)

# Interested in publishing with us?
# Contact book.department@intechopen.com

# Designer Laser Resonators based on Amplifying Photonic Crystals

Alexander Benz[1], Christoph Deutsch[1], Gernot Fasching[1], Karl Unterrainer[1],
Aaron M. Maxwell[2], Pavel Klang[2], Werner Schrenk[2] and Gottfried Strasser[2]
*[1]Photonics Institute and Centre for Micro- and Nanostructures,*
*Vienna University of Technology*
*[2]Institute of Solid-State Electronics and Centre for Micro- and Nanostructures,*
*Vienna University of Technology*
*Austria*

## 1. Introduction

The design and realisation of lasers involves two main steps: the development of the gain medium and the development of the optical resonator. Naturally, both have a major impact on the device performance. The light that passes through the active medium and lies within a certain frequency range is amplified. The resonator confines the light and defines the way it travels through the gain medium.

The focus of the present work is the design and realisation of micro resonators based on photonic crystals (PhCs). The key feature of PhCs is the possibility to design the dispersion relation for electromagnetic waves by patterning on a wavelength scale Joannopoulus et al. (2008). The optical properties of the resonator can be manipulated without almost any restrictions. Essential device parameters such as emission frequency, lasing far-field or cavity quality-factor (Q-factor) are balanced simultaneously. The PhCs are incorporated directly into the active region of a terahertz (THz) quantum-cascade laser (QCL) Köhler et al. (2002). The use of THz-QCLs allows for an easy experimental realisation of the desired resonator geometry. The large emission wavelength on the order of 100 $\mu$m allows for a simple processing using optical lithography and sets high tolerances for the fabrication.

We present two different schemes for PhC laser resonators in theory and experiment. The first one uses a bulk active region which is surrounded by a PhC-mirror. The light is confined by the mirror and amplified in the central gain region. The spatial separation of the two main laser components allows for a simpler fabrication. However, it comes at the expense of larger devices. The second resonator type uses the PhC directly as the gain medium. It is fabricated from the active region of a THz-QCL, making the bulk gain region redundant. The device performance is greatly enhanced in terms of emission frequency control.

## 2. Active region of the THz quantum-cascade lasers

The basic building block of every QCL is a superlattice, materials with different bandgaps are grown on top of each other. If the thickness of the individual layers is in the range of a

few nm's, a further quantisation of the electron states can be achieved. The theoretical fundamentals are from the 1970's mainly by R. Tsu and L. Esaki Tsu & Esaki (1973); Tsu et al. (1974). The idea to use intersubband transitions as an active laser medium has been proposed in 1971 by R. F. Kazarinov and R. A. Suris Kazarinov & Suris (1971). The essential point is the possibility to design the electron wave functions by carefully selecting the thickness of the individual layers. We are able to control all the parameters in the active region, such as the dipole matrix element, the upper state life time or the transition energy independently of the used material system. All these parameters become independent of the used material system. To increase the gain further, identical cascades are grown on top of each other. Electrons from the ground state in one cascade are injected into the upper laser state of the next cascade, allowing for electron recycling. All these advantages and the opportunities in design have made QCLs the preferred monolithic source in the MIR and THz spectral region, covering wavelengths from 3 to 300 $\mu$m.

The physical nature of the QCLs has another direct consequence, which is essential for this work. QCLs are unipolar devices, only one carrier type is involved in the current transport and the light generation. This makes QCLs insensitive to surface effects allowing for the realization of almost any resonator geometry. In contrast, the light generation in classical bandgap lasers is based on an electron-hole recombination across the bandgap. Therefore, an increase in device surface leads to a strong increase in surface leakage currents which in the end limits the device performance.

The active region we are using is based on a gallium-arsenide (GaAs) / aluminium-gallium-arsenide (AlGaAs) heterostructure. The barriers have an Al-content of 15 % leading to a typical height of 110 meV. A calculated bandstructure at lasing field is shown in Fig. 1(a), one cascade consists of only four wells. The optical transition in this design is vertical, leading to stronger coupling of the upper and lower laser state and reduced sensitivity to interface roughness. The 2.7 nm thin barrier, in between the double well, has the strongest influence on the transition energy. An increased thickness leads to a red-shift in the emission frequency as the anti-crossing between the upper and lower laser states is reduced.
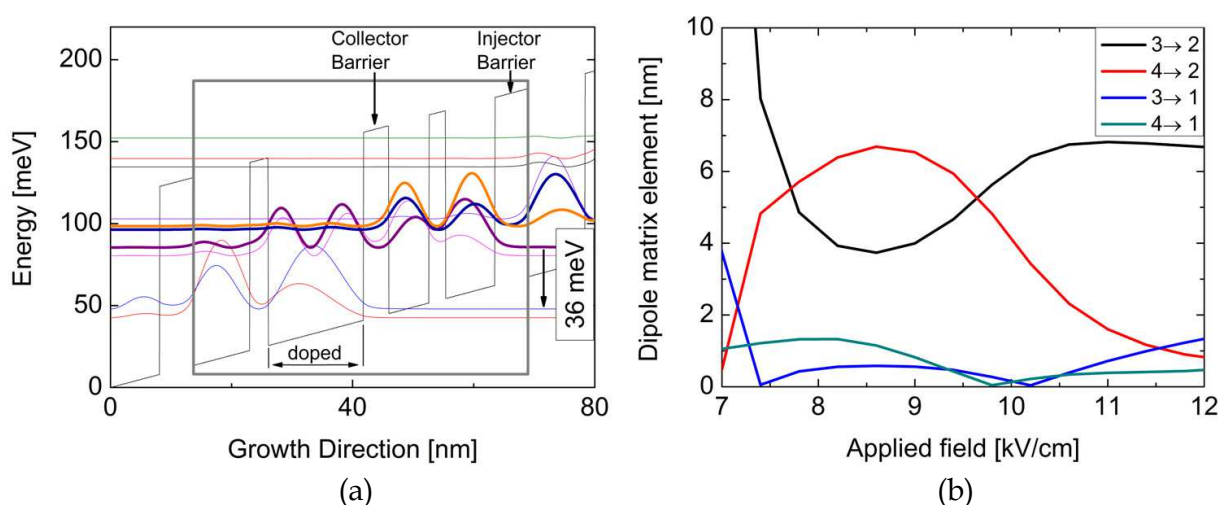


Fig. 1. (a) Calculated bandstructure at the lasing field of 9.8 kV/cm. The lasing states are marked with bold lines (purple=2, blue=3, orange=4). One cascade is marked with the grey box. (b) Field dependence of the dipole matrix elements. Only the transitions 3→2 and 4→2 have a relevant coupling strength, the other transitions are optically not active.

The lower laser state is depopulated via a resonant LO phonon emission allowing us to achieve scattering times of around 0.5 ps Williams et al. (2002). Thereby, a stable population inversion can be achieved. The large separation of 36 meV between the lower laser state and the ground state reduces the thermal back filling strongly. Nevertheless, the operating temperature of THz-QCLs is still limited to cryogenic levels. The highest operating temperature reported currently is 186 K Kumar et al. (2009).

One should keep in mind that the optical parameters of the active region depend on the applied field. The coupling strength between the upper and the lower laser state varies with the field. For values below 9.5 kV/cm the transition $4 \rightarrow 2$ is the dominant one, for higher fields $3 \rightarrow 2$, as illustrated in Fig. 1(b). The emission energy shows a blue-shift with increasing field for all the transitions due to the Stark effect. A larger applied field leads to a stronger separation of the electron states.

## 3. Plasmonic waveguides

The waveguide is responsible for the confinement of the optical mode, it guarantees the overlap with the gain region. For traditional bandgap lasers, waveguides based on total internal reflection are used. The gain region has a higher refractive index than the surrounding medium. However, this concept only works for waveguide thicknesses larger than the optical wavelength involved. For THz-QCLs this is almost impossible to achieve. The wavelengths are in the range of 60 to 300 $\mu$m in general. With the available growth techniques such as molecular beam epitaxy or metal-organic chemical vapour deposition, it is not practical to grow a heterostructure with the desired thickness and still to maintain the precision required. Typically, we are limited to 10 or 15 $\mu$m thick heterostructures. Such waveguides cannot rely on total internal reflection. The solution is the use of plasmonic waveguides.

To be more precise, the waveguides for THz-QCLs rely on surface plasmons. As any other surface wave, surface plasmons are bound to an interface and decay exponentially into both media. For propagation, it is necessary that the refractive index has different sign on both sides of the interface. A conventional semiconductor which is undoped or low doped has a positive refractive index. Metals or highly doped semiconductors, which act quasi-metallic, have a negative refractive index in the THz spectral region. Therefore, if the active region is sandwiched between two, thin metallic or quasi-metallic layers, an efficient waveguide is formed. This concept is well known from the microwave technology, where micro strip waveguides are used successfully Käs & Pauli (1991).

In this work we use the so-called double-metal (DM) waveguide Kohen et al. (2005). The entire structure consists of two gold layers and the active region in between. For an electrical contact between the metal and the semiconductor we use 100 nm thin highly doped n+-contact layers. As the THz-mode hardly penetrates the metal, a confinement of almost 100 % is realised. Simulations for a 15 $\mu$m thin and 100 $\mu$m wide DM waveguide are shown in Fig. 2. As the waveguide is much thinner the wavelength, only the first order mode in vertical direction can propagate. This mode shows an almost constant mode profile along the vertical axes. It has to be stressed that also the lateral confinement is excellent. The mode hardly leaks out of the waveguide into the surrounding air. Another advantage is the high reflectivity of 90 % for untreated facets due to the impedance mismatch between the waveguide and the free space Maineult et al. (2008).
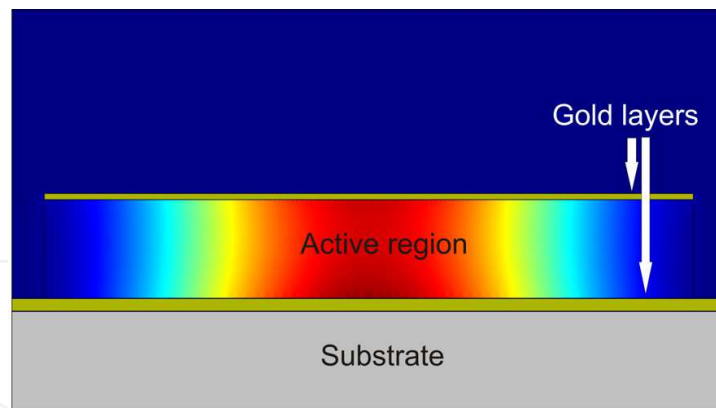
Fig. 2. Two-dimensional simulation of a DM waveguide using *Comsol Multiphysics* (www.comsol.com). The mode profile is almost constant in the vertical direction. Despite the finite width of the ridge, there is no significant leakage in the lateral direction.

## 4. Photonic crystal theory

Section 2 described the design of the active region itself. The heterostructure designed can be interpreted as artificial crystal for electrons manipulating the electron wave functions. PhCs on the other hand can be seen as artificial crystals for light. The full dispersion relation for electromagnetic waves becomes designable. The combination of QCLs and PhCs allows us to design all aspects of the laser in terms of gain medium and optical resonator.

### 4.1 Mathematical description of photonic crystals

We will describe the optical properties for a classical system, the quantisation of the electromagnetic field can be neglected in this case. We use the Maxwell's Equations Jackson (1999) with some significant simplifications.

- There are no free charges or currents present in the system.
- We restrict ourselves to purely dielectric media: dispersion is neglected, non-linearity is neglected, the refractive index is independent of time and the relative permeability is set to 1. Therefore, we are able to write the relative permittivity $\epsilon(\vec{r})$ solely as a function of position.
- The involved fields vary harmonically in time, which allows us to replace any derivative in respect to time $\partial/\partial t$ by $-i\omega$.

All this simplifications allows us to decouple the Maxwell's Equation resulting in two independent equations for the electric field $\vec{E}(\vec{r})$ and for the magnetic field $\vec{H}(\vec{r})$

$$\nabla \times \left( \frac{1}{\epsilon(\vec{r})} \nabla \times \vec{H}(\vec{r}) \right) = \left( \frac{\omega}{c} \right)^2 \vec{H}(\vec{r}), \tag{1}$$

$$\nabla \times \nabla \times \vec{E}(\vec{r}) = \left( \frac{\omega}{c} \right)^2 \epsilon_r(\vec{r}) \vec{E}(\vec{r}). \tag{2}$$

For mathematical convenience normally the equation for the magnetic field is solved and then used to calculate the electric field. We want to obtain the solution for the PhC, which is a periodic system. According to Bloch's Theorem, the solution has to have the same periodicity as the crystal, giving us the basic solution to our problem:

$$\vec{H}_k = exp\left(i\vec{k}\cdot\vec{r}\right)\vec{u}_k\left(\vec{r}\right), \tag{3}$$

where $\vec{k}$ is the Bloch wave vector and $\vec{u}_k\left(\vec{r}\right)$ the so-called Bloch function. We know that almost any periodic function can be written as a sum of harmonic functions. This defines the basic form for our unknown Bloch function:

$$\vec{u}_k\left(\vec{r}\right) = \sum_G \vec{c}_G\left(\vec{k}\right) exp\left(i\vec{G}\cdot\vec{r}\right), \tag{4}$$

where $\vec{G}$ is the sum over all reciprocal lattice vectors and $\vec{c}_G$ are the Fourier coefficients. After lengthy calculations, we have simplified a set of partial differential calculations into a set of linear equations. Now the Fourier coefficients become accessible:

$$\sum_G -\epsilon_{G'-G}^{-1}\cdot\left(\vec{k}+\vec{G'}\right)\times\left(\vec{k}+\vec{G}\right)\times\vec{c}_G = \frac{\omega^2}{c^2}\vec{c}_{G'}. \tag{5}$$

The Fourier transform of the inverse dielectric function $\epsilon_G^{-1}$ can be calculated very efficiently with the Fast-Fourier Transformation giving us an easy-to-use tool for the design of PhCs.

### 4.2 Limitations of the mathematical description

As already mentioned, due to all these simplifications the results are valid only for 'perfect' systems. The PhC is infinitely large and consists of perfectly linear and loss-less materials. However, these limitations are not very critical for our devices. Due to the excellent coupling between the mode and PhC, even a small resonator behaves similar to the ideal PhC. The frequency dependent gain can be implemented by perturbation theory using a complex permittivity in the form $\epsilon = \epsilon' + i\delta$. For realistic THz-QCL it is not even necessary as the error due to the gain is negligible Nojima (1998b).

### 4.3 Design of photonic crystals

The PhC used for the resonator experiments has always the same basic structure, a schematic is shown in Fig. 3(a). It consists of isolated, free-standing pillars which are surrounded by air. Such structures typically show full bandgaps for TM-polarised light Johnson et al. (1999), which is the polarisation of light emitted by a QCL. The PhC is embedded in a DM waveguide for the real devices. For the simulations we use 2D simulations of infinitely high rods which significantly reduces the computational effort. As the waveguide allows only one vertical mode with an almost constant mode profile to propagate, there is virtually no dependence in the vertical direction. Experiments by Schartner et al. (2006) show that 2D-PhCs in plasmonic waveguides can be simulated using only 2D simulations and achieving very accurate results.

We use a ratio r/a of 0.3 for the calculations, where r is the radius of the pillars and a the period of the PhC. The refractive index for the pillars is set to 3.65, an experimental value for GaAs at 3 THz Yasuda & Hosako (2008). For now, the system is set ideal, i.e. the system is loss-less and infinitely large. The calculated bandstructure in Fig. 3(b) shows the expected full bandgaps for TM-modes. The first one spans from 0.21 to 0.3 [fa/c], the second one from 0.39 to 0.51 [fa/c], where f is the frequency and c the speed of light. Frequencies which lie inside the bandgap cannot propagate through the PhC. The only possible solution for the

Maxwell's Equations are waves with a complex $\vec{k}$-vector, in other words exponentially decaying waves.



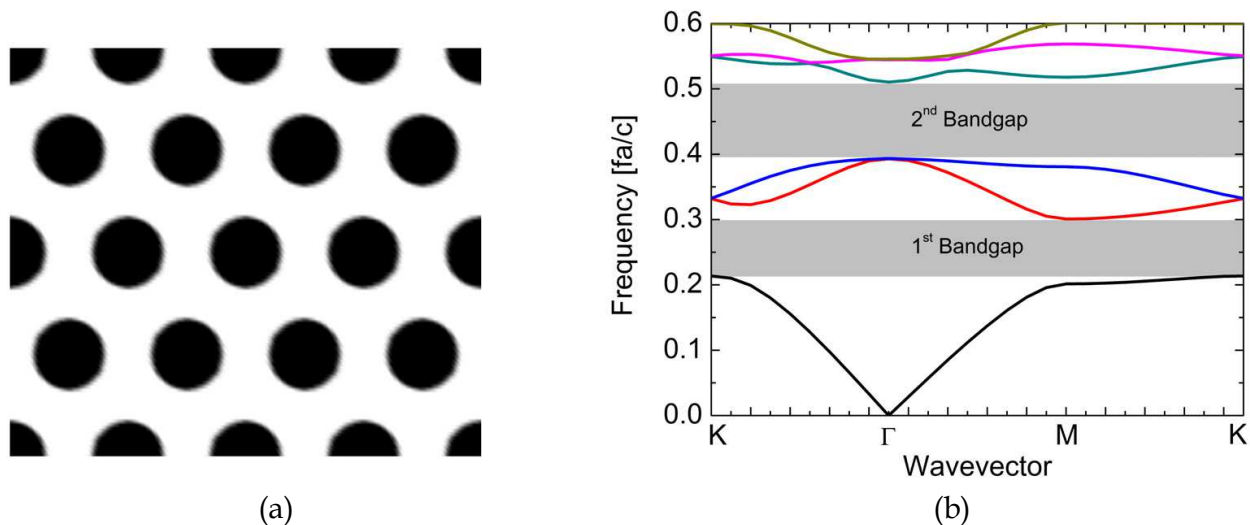(a)                                                                    (b)

Fig. 3. (a) Schematic of the PhC used. The isolated high-index pillars are arranged in a hexagonal lattice and surrounded by air. (b) The band structure for the ideal PhC. The first eight bands are presented, the full bandgaps for TM-polarised light are clearly visible.

## 5. Photonic crystal mirror devices

The first set of devices consists of two parts, a bulk gain region is surrounded by a PhC mirror. A schematic of the resonator is illustrated in Fig. 4. The PhC works as a frequency selective mirror allowing for tuning the emission frequency from the gain maximum into the bandgap of the PhC. The parameters of the PhC are identical to the previous section. The period is varied from 22 to 35 μm while r/a is 0.3. The entire device is embedded into a DM waveguide ensuring a strong interaction between the mode inside the gain region and inside the PhC. The thickness of the waveguide is equal for the different periods, it is defined by the thickness of the active region of 15 $\mu$m.

### 5.1 Simulation results for photonic crystal mirrors

For the simulation of the real device, the plane-wave expansion method (PWE) method is not well suited. The bulk gain region can be seen as a defect which breaks the periodicity of the PhC. So-called 'super-cells' allow for an incorporation of the defect while maintaining periodic boundaries by an artificial increase of the computational cell. However, the artificial increase leads to band folding, the number of possible bands is increased making the identification of individual bands difficult Feng & Arakawa (1997); Kuzmiak & Maradudin (1998); Zhi et al. (2003).

To avoid these problems FDTD-calculations using the open-source package *MIT Electromagnetic Equation Propagation* (MEEP) are performed for our resonators Farjadpour et al. (2006). We restrict ourselves again to 2D-simulations of a hexagonal core which is surrounded by two rows of pillars. The core is large enough to support modes on its own. Therefore, we have also simulated reference cavities consisting of only the core, the pillars have been removed. Now the modes visible can be assigned either to the hexagonal cavity
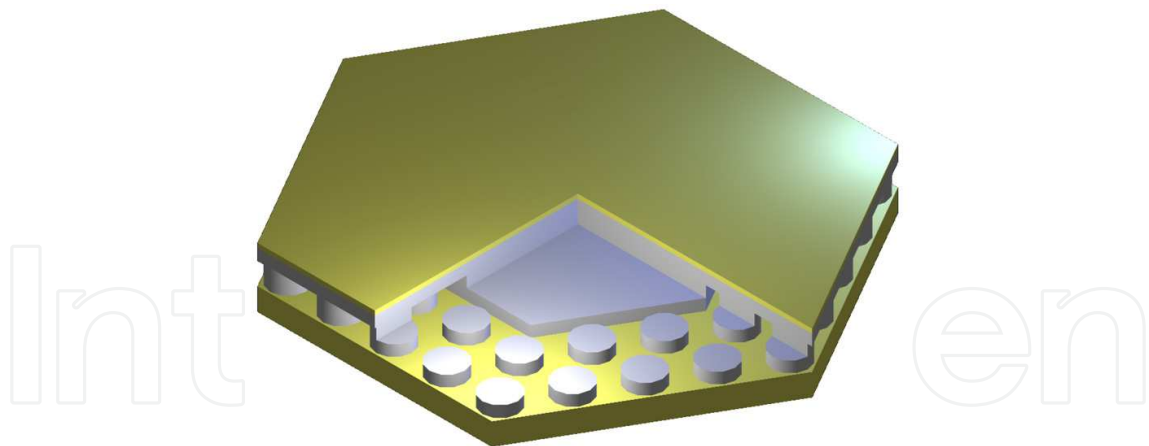
Fig. 4. Schematic of the PhC-mirror device Benz et al. (2007). The bulk gain region is surrounded by a PhC which acts as a frequency selective mirror. The device is embedded in a DM-waveguide to ensure a strong modal coupling between the gain region and the PhC.
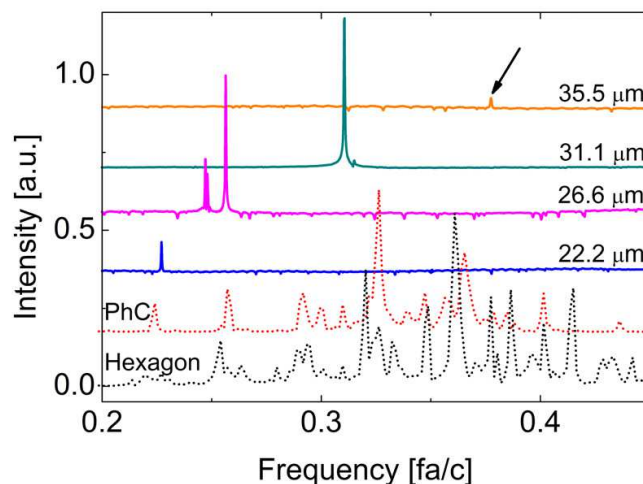


Fig. 5. Simulated and measured spectra for the PhC-mirror devices Benz, Deutsch, Fasching, Unterrainer, Andrews, Klang, Schrenk & Strasser (2009). The dotted lines represent simulations for the bare cavity and the full device respectively. The solid lines show measured spectra for different periods of the PhC.

or to the PhC. The calculated spectra in Fig. 5 show clearly that additional modes appear due to the PhC. For higher frequencies, the number of possible modes increases strongly, as the wavelength becomes smaller while the resonator size remains unchanged. Due to the strong optical coupling with the PhC, it is enough to use only two rows of pillars to achieve the frequency control.

### 5.2 Experimental results for photonic crystal mirrors

We have used the same active region to process devices with different periods, the corresponding spectra are shown in Fig. 5. The predicted modes are clearly visible in the measurements, corresponding to frequencies of 0.224, 0.256, 0.309 and 0.378 [fa/c]. One should keep in mind that the exact position of the frequencies also depends on the size of the core as the geometric path is changed for the modes. Nevertheless, the mode position overlaps nicely with the calculated bandgaps. This behaviour is expected, as the PhC-

mirrors shows the lowest losses for frequencies within the bandgap. The devices do not show single-mode emission, in general, as broad stop bands are used. Due to the inhomogeneously broadened gain with a typical full-width at half-maximum (FWHM) gain bandwidth of 130 GHz, multi-mode emission becomes easily possible Kröll et al. (2007).

The device with a period of 31.05 $\mu$m has to be treated separately from the other devices. The laser emits between the first two bandgaps at 0.31 [fa/c]. This corresponds to a mode at the K-point. Such modes at high symmetry point appear at flat-band regions in the PhC-bandstructure due to very low group velocity. The long interaction time with the PhC results in strong feedback. These regions are especially interesting for resonators without any bulk gain region. As they do not require any states inside the bandgap and still allow for an excellent frequency selection.

## 6. Active photonic crystal laser

The last resonator type that we are going to investigate is based purely on isolated pillars. The specifications for the PhC are identical to the previous sections, the same PhC geometry, ratio $r/a$, refractive index and waveguide. It is important to stress that now the bulk gain region has been removed, as shown in Fig. 6. The sub-wavelength, isolated pillars have to provide the optical feedback and the required gain. The pillars are fabricated directly from the active region of a THz-QCL and again embedded in a DM waveguide. Thereby, we are able to achieve a very simple and efficient pumping scheme. Only the pillars underneath the top contact are pumped and the electric field distribution is perfectly homogeneous.
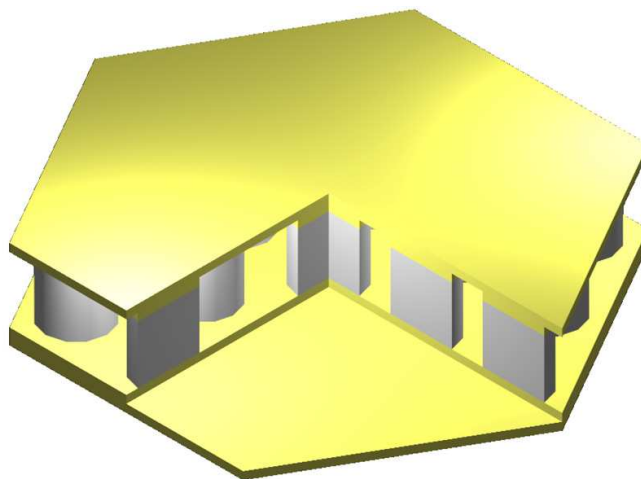


Fig. 6. Schematic of the active PhC laser Benz, Deutsch, Fasching, Andrews, Unterrainer, Klang, Schrenk & Strasser (2009). The pillars are fabricated directly from the active region of a THz-QCL, there is no need for an additional bulk gain region. This type of cavity relies on PhC band edges rather than on defect states.

### 6.1 Simulation results for active photonic crystals

As there is no defect incorporated, the real device is very close to the ideal PhC. The only limitation is the finite size which will be treated later. Starting from the PWE calculations we see immediately that lasing inside the bandgap is not possible as there are no allowed states. Lasing will occur at the flat band region at the K-point. However, to establish lasing at all it

is important to know the mode distribution inside the resonator. It is easy to calculate the electric field for the ideal PhC. The corresponding energy distribution shows that 95 % of the modal energy overlaps with the active pillars. This is necessary as only the pillars are pumped, the surrounding air is, in the best case, transparent. The high modal overlap in combination with the strongly reduced group velocity is predicted to give strong gain enhancement in this type of structure Nojima (2001; 1998a); Sakoda (1999).

According to simulations, finite size arrays of isolated pillars support lasing modes on their own without the need for any further mirrors Nojima (1999). For our FDTD-calculations we arranged 37 pillars in a hexagonal shape. Even this small number of pillars already supports a few lasing modes, the calculated spectrum is shown in Fig. 7(a). The mode at 0.19 [fa/c] corresponds to the M-point and has a Q-factor of 60, the one at 0.21 [fa/c] to the K-point and has a Q-factor of 1000. For frequencies above 0.3 [fa/c] additional modes corresponding to higher lying bands show up. In between, the PhC bandgap is nicely visible. These calculations predict that these devices should operate in stable single-mode emission at the K-point. One should keep in mind that the simulations overestimate the Q-factor of the real device. The main limitation is the loss in the gold and the thin n+-layers. These effects are naturally ignored in the 2D-simulations. The reduction of the Q-factor due to interface roughness, which normally limits the Q-factor for PhC in the visible Asano et al. (2006); Srinivasan & Painter (2002; 2003), is not a problem as the processing imperfections are much smaller than the wavelength.

### 6.2 Experimental results for active photonic crystals

As expected, the devices show a stable single-mode emission defined by the PhC. Fig. 7(a) shows the emission of devices with a 26.6 and 31.1 $\mu$m period respectively. Both devices are lasing around 0.23 [fa/c] which corresponds to the K-point or the mode with the significantly higher Qfactor. We attribute the discrepancy between experiment and simulation to imperfections in the processing, uncertainties in the refractive index of the active region and the effects of the DM waveguide.

Apart from the possibility to predict the emission frequency, one should keep in mind that this concept shows a huge tuning range for lasing. The devices with a 26.62 $\mu$m period are lasing at 2.56 THz, which corresponds almost to the gain maximum of 2.6 to 2.7 THz Benz, Deutsch, Fasching, Andrews, Unterrainer, Klang, Schrenk & Strasser (2009). Using a 31.05 $\mu$m period shifts the emission frequency to 2.25 THz. Spectra for both devices at different applied fields are shown in Fig. 7(b). This corresponds to a possible tuning range of 400 GHz which is significantly larger the typical FWHM gain bandwidth of THz-QCLs of only 130 GHz Kröll et al. (2007). This is a strong evidence for the theoretically predicted gain enhancement in this type of structures. Additionally, it also shows the large potential for this kind of resonator. It combines an excellent frequency control with a huge tuning range.

## 7. Conclusion

The design and the realisation of laser resonators is a challenging task. In general, it is necessary to balance aspects such as quality factor, laser far-field, threshold and output power. Incorporating PhCs allows for a full control of the dispersion relation of the resonator. This new flexibility can be used to fulfil all the requirements at the same time.
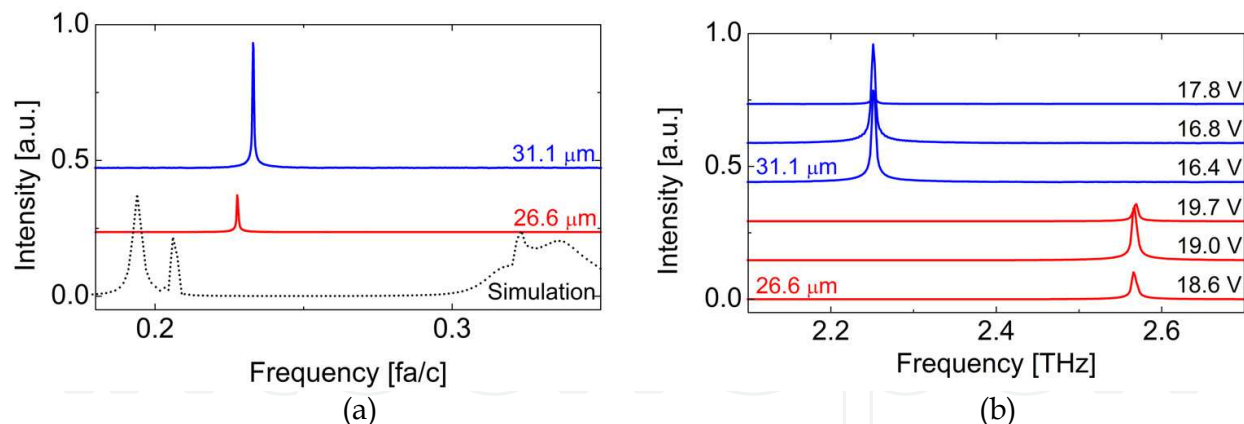
Fig. 7. (a) Simulated and recorded spectra for the active PhC laser Benz, Deutsch, Fasching, Andrews, Unterrainer, Klang, Schrenk & Strasser (2009). The realised devices are both lasing at the K-point, close to the predicted emission frequency. (b) Measured spectra for different periods of the PhC as a function of the applied bias. Both devices show a stable single-mode emission which is independent of the voltage.

Here, we have presented the design of PhCs for THz-QCLs, which are an ideal system to study the behaviour experimentally. The large wavelength allows for simple processing and large tolerances. The unipolar nature of QCLs makes the devices insensitive to surface leakage. Therefore, it is possible to directly integrate the PhC into the active laser medium.

The devices presented can be split into two different concepts. The first type of devices are based on PhC mirrors. A bulk gain region is surrounded by a PhC mirror. The emission of the device is tuned into the bandgap of the PhC, corresponding to the lowest mirror losses. These devices show a multi-mode emission in general due to the broad stop bands used. Nevertheless, this is an easy concept to be realised. The second type of devices consists of the active pillars only, there is no bulk gain region. The sub-wavelength pillars are used to create the required gain and the optical feedback. The strong modal confinement in lateral and vertical directions allows us to built resonators with dimension comparable to the emission wavelength. The excellent optical properties of the resonator also allow us to achieve a tuning range of 400 GHz, which is significantly wider than the typical FWHM gain bandwidth of THz-QCLs of only 130 GHz. In addition, the number of modes can be reduced significantly as narrow band edges are used which are surrounded by wide forbidden bands.

The simulations are in excellent agreement with the experimental results. We are able to precisely predict the emission frequencies for both types of cavities. Using the PWE method, we can determine the band structure of the ideal crystal including the position of the bandgaps. The group velocity and the modal overlap for any mode can be calculated. The FDTD-simulations allow us to simulate the entire resonator. There are no restrictions on the symmetry of the resonator or the linearity of the used materials. One simulation run generates the entire frequency information. The Q-factors can be determined easily. Especially for lower frequencies and smaller devices, the predictions are excellent, as the number of possible modes remains limited.

## 8. References

Asano, T., Song, B.-S. & Noda, S. (2006). Analysis of experimental q factors (~1 million) of photonic crystal nanocavities, *Opt. Express* 14: 1996.

Benz, A., Deutsch, C., Fasching, G., Andrews, A. M., Unterrainer, K., Klang, P., Schrenk, W. & Strasser, G. (2009). Active photonic crystal terahertz laser, *Opt. Express* 17: 941.

Benz, A., Deutsch, C., Fasching, G., Unterrainer, K., Andrews, A. M., Klang, P., Schrenk, W. & Strasser, G. (2009). Photonic crystal mode terahertz lasers, *J. Appl. Phys.* 105: 122404.

Benz, A., Fasching, G., Deutsch, C., Andrews, A. M., Unterrainer, K., Klang, P., Schrenk, W. & Strasser, G. (2007). Terahertz photonic crystal resonators in double-metal waveguides, *Opt. Express* 15: 12418.

Farjadpour, A., Roundy, D., Rodriguez, A., Ibanescu, M., Bermel, P., Joannopoulos, J. D., Johnson, S. G. & Burr, G. (2006). Improving accuracy by subpixel smoothing in fdtd, *Opt. Lett.* 31: 2972.

Feng, X.-P. & Arakawa, Y. (1997). Defect modes in two-dimensional triangular photonic crystals, *Jpn. J. Appl. Phys.* 36: 120.

Jackson, J. D. (1999). *Classical Electrodynamics*,Wiley, New York.

Joannopoulus, J. D., Johnson, S. G., Winn, J. N. & Meade, R. D. (2008). *Photonic crystals - Molding the flow of light*, Princeton University Press.

Johnson, S. G., Fan, S., Villeneuve, P. R., Joannopoulos, J. D. & Kolodziejski, L. A. (1999). Guided modes in photonic crystal slabs, *Phys. Rev. B* 60: 5751.

Käs, G. & Pauli, P. (1991). *Mikrowellentechink - Grundlage, Anwendungen, Messtechnik*, Franzis Verlag Gmbh, München.

Kazarinov, R. F. & Suris, R. A. (1971). Possibility of amplification of electromagnetic waves in a semiconductor with a superlattice, *Fizika i Tekhnika Poluprovodnikov* 5: 797.

Kohen, S., Williams, B. S. & Hu, Q. (2005). Electromagnetic modeling of terahertz quantum cascade laser waveguides and resonators, *J. Appl. Phys.* 97: 053106.

Köhler, R., Tredicucci, A., Beere, H., Lienfield, E., Davis, A., Ritchie, D., Iotti, R. & Rossi, F. (2002). Terahertz semiconductor heterostructure laser, *Nature (London)* 417: 156.

Kröll, J., Darmo, J., Dhillon, S. S., Marcadet, X., Calligaro, M., Sirtori, C. & Unterrainer, K. (2007). Phase-resolved measurements of stimulated emission in a laser, *Nature (London)* 449: 698.

Kumar, S., Hu, Q. & Reno, J. L. (2009). 186 K operation of terahertz quantum-cascade lasers based on a diagonal design, *Appl. Phys. Lett.* 94: 131105.

Kuzmiak, V. & Maradudin, A. A. (1998). Localized defect modes in a two-dimensional triangular photonic crystal, *Phys. Rev. B* 57: 15242.

Maineult, W., Gellie, P., Andronico, A., Filloux, P., Leo, G., Sirtori, C., Barbieri, S., Peytavit, E., Akalin, T., Lampin, J.-F., Beere, H. E., & Ritchie, D. A. (2008). Metal-metal terahertz quantum cascade laser with micro-transverse-electromagnetic-horn antenna, *Appl. Phys. Lett.* 93: 183508.

Nojima, S. (1998a). Enhancement of optical gain in two-dimensional photonic crystals with active lattice points, *Jpn. J. Appl. Phys.* 37: 565.

Nojima, S. (1998b). Polarization anisotropy of optical gain in two-dimensional photonic crystals with active lattice point, *Jpn. J. Appl. Phys.* 37: 6418.

Nojima, S. (1999). Single-mode laser oscillation in semiconductor gain photonic crystals, *Jpn. J. Appl. Phys..* 38: 867.

Nojima, S. (2001). Optical-gain enhancement in two-dimensional active photonic crystals, *J. Appl. Phys.* 90: 545.

Sakoda, K. (1999). Enhanced light amplification due to group-velocity anomaly peculiar to two- and three-dimensional photonic crystals, *Opt. Express* 4: 167.

Schartner, S., Golka, S., Pflügl, C., Schrenk,W., Andrews, A. M., Roch, T. & Strasser, G. (2006). Band strucuture mapping of photonic crystal intersubband detectors, *Appl. Phys. Lett.* 89: 151107.

Srinivasan, K. & Painter, O. (2002). Momentum space design of high-q photonic crystal optical cavities, *Opt. Express* 10: 670.

Srinivasan, K. & Painter, O. (2003). Fourier space design of high-q cavities in standard and compressed hexagonal lattice photonic crystals, *Opt. Express* 11: 579.

Tsu, R. & Esaki, L. (1973). Tunneling in finite superlattice, *Appl. Phys. Lett.* 22: 562.

Tsu, R., Koma, A. & Esaki, L. (1974). Optical properties of semiconductor superlattice, *J. Appl. Phys.* 46: 842.

Williams, B., Callebaut, H., Kumar, S., Hu, Q. & Reno, J. (2002). 3.4 thz quantum cascade laser based on longitudinal-optical-phonon scattering for depopulation, *Appl. Phys. Lett.* 82: 1015.

Yasuda, H. & Hosako, I. (2008). Measurement of terahertz refractive index of metal with terahertz time-domain spectroscopy, *Jpn. J. Appl. Phys.* 47: 1632.

Zhi, W., Guobin, R., Shuqin, L. & Shuishend, J. (2003). Supercell lattice method for photonic crystal fibers, *Opt. Express* 11: 980.
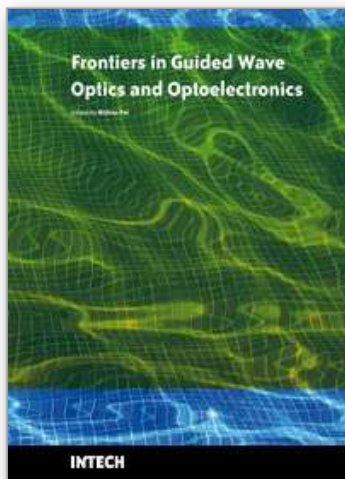
**Frontiers in Guided Wave Optics and Optoelectronics**

Edited by Bishnu Pal

ISBN 978-953-7619-82-4

Hard cover, 674 pages

**Publisher** InTech

**Published online** 01, February, 2010

**Published in print edition** February, 2010

As the editor, I feel extremely happy to present to the readers such a rich collection of chapters authored/co-authored by a large number of experts from around the world covering the broad field of guided wave optics and optoelectronics. Most of the chapters are state-of-the-art on respective topics or areas that are emerging. Several authors narrated technological challenges in a lucid manner, which was possible because of individual expertise of the authors in their own subject specialties. I have no doubt that this book will be useful to graduate students, teachers, researchers, and practicing engineers and technologists and that they would love to have it on their book shelves for ready reference at any time.

**How to reference**

In order to correctly reference this scholarly work, feel free to copy and paste the following:

Alexander Benz, Christoph Deutsch, Gernot Fasching, Karl Unterrainer, Aaron M. Maxwell, Pavel Klang, Werner Schrenk and Gottfried Strasser (2010). Designer Laser Resonators based on Amplifying Photonic Crystals, Frontiers in Guided Wave Optics and Optoelectronics, Bishnu Pal (Ed.), ISBN: 978-953-7619-82-4, InTech, Available from: http://www.intechopen.com/books/frontiers-in-guided-wave-optics-and-optoelectronics/designer-laser-resonators-based-on-amplifying-photonic-crystals

# INTECH
open science | open minds